AMERICAN COLLEGE
of RHEUMATOLOGY
Empowering Rheumatology Professionals

Antibodies to Cartilage Oligomeric Matrix Protein Are Pathogenic in Mice and May Be Clinically Relevant in Rheumatoid Arthritis

Changrong Ge,[1] 🆔 Dongmei Tong,[1] Erik Lönnblom,[1] Bibo Liang,[2] Weiwei Cai,[1] Cecilia Fahlquist-Hagert,[3] 🆔 Taotao Li,[1] Alf Kastbom,[4] 🆔 Inger Gjertsson,[5] Doreen Dobritzsch,[6] and Rikard Holmdahl[2] 🆔

Objective. Cartilage oligomeric matrix protein (COMP) is an autoantigen in rheumatoid arthritis (RA) and experimental models of arthritis. This study was undertaken to investigate the structure, function, and relevance of anti-COMP antibodies.

Methods. We investigated the pathogenicity of monoclonal anti-COMP antibodies in mice using passive transfer experiments, and we explored the interaction of anti-COMP antibodies with cartilage using immunohistochemical staining. The interaction of the monoclonal antibody 15A11 in complex with its specific COMP epitope P6 was determined by x-ray crystallography. An enzyme-linked immunosorbent assay and a surface plasma resonance technique were used to study the modulation of calcium ion binding to 15A11. The clinical relevance and value of serum IgG specific to the COMP P6 epitope and its citrullinated variants were evaluated in a large Swedish cohort of RA patients.

Results. The murine monoclonal anti-COMP antibody 15A11 induced arthritis in naive mice. The crystal structure of the 15A11–P6 complex explained how the antibody could bind to COMP, which can be modulated by calcium ions. Moreover, serum IgG specific to the COMP P6 peptide and its citrullinated variants was detectable at significantly higher levels in RA patients compared to healthy controls and correlated with a higher disease activity score.

Conclusion. Our findings provide the structural basis for binding a pathogenic anti-COMP antibody to cartilage. The recognized epitope can be citrullinated, and levels of antibodies to this epitope are elevated in RA patients and correlate with higher disease activity, implicating a pathogenic role of anti-COMP antibodies in a subset of RA patients.

INTRODUCTION

Rheumatoid arthritis (RA) is a chronic autoimmune disease characterized by inflammation and damage in synovial joints. It affects 0.5–1% of the population worldwide (1–3). RA is caused by a complex set of genes and environmental factors, although none of these have been firmly defined or functionally understood (4–6). There is increasing evidence that environmental exposures, such as silica dust, bacterial stimuli, and tobacco smoking, cause chronic mucosal inflammation, possibly contributing to RA development (7–9). However, the mechanisms by which chronic inflammation triggers adaptive autoimmunity, in particular a B cell response to citrullinated proteins and later toward joint proteins, are not yet well understood (10).

Cartilage oligomeric matrix protein (COMP) is a noncollagenous matrix glycoprotein that belongs to the thrombospondin family of extracellular calcium-binding proteins (11). It is predominantly expressed in cartilage and is also found in other tissue, such as tendons, bones, blood vessels, and synovial membrane (12). COMP is a pentameric protein with each monomer consisting of an N-terminal domain followed by 4 epidermal growth factor (EGF)–like domains, 8 type III thrombospondin domains, and a C-terminal globular domain (13). The specific function of COMP is still undefined, but it appears to play a structural role in the assembly and

[1]Changrong Ge, PhD, Dongmei Tong, PhD, Erik Lönnblom, PhD, Weiwei Cai, PhD, Taotao Li, PhD: Karolinska Institute, Stockholm, Sweden; [2]Bibo Liang, PhD, Rikard Holmdahl, MD, PhD: Karolinska Institute, Stockholm, Sweden, and Southern Medical University, Guangzhou, China; [3]Cecilia Fahlquist-Hagert, PhD: Karolinska Institute, Stockholm, Sweden, and University of Turku, Turku, Finland; [4]Alf Kastbom, MD, PhD: Linköping University, Linköping, Sweden; [5]Inger Gjertsson, MD, PhD: University of Gothenburg, Gothenburg, Sweden; [6]Doreen Dobritzsch, PhD: Uppsala University, Uppsala, Sweden.
Address correspondence to Rikard Holmdahl, MD, PhD, Biomedicum, Quarter 9D Solnavägen 9, Solna, Sweden. Email: rikard.holmdahl@ki.se.

stabilization of the extracellular matrix (ECM) through its interactions with collagen fibrils and other matrix components, such as proteoglycans and fibronectin (14).

The functional importance of COMP in cartilage is indicated by its association with several joint diseases (14). As a marker of cartilage turnover, elevated COMP levels are found in the serum and synovial fluid from patients with joint diseases such as RA and osteoarthritis (OA) (15). Because it reflects the specific metabolic activities of cartilage tissue, it has been suggested that COMP is a potential diagnostic and prognostic biomarker in joint diseases (15). Interestingly, circulating COMP fragments bind C3b and could be both an inhibitor and an initiator of complement activation in RA, but not in OA (16).

Cartilage damage and degradation in chronic joint disease are believed to promote an autoimmune reaction to cartilage components. We previously demonstrated that homologous COMP could induce arthritis in certain animal strains, highlighting its pathogenic role in experimental arthritis (17,18). In addition, disease can be transferred from arthritic mice to healthy recipients via affinity-purified COMP-specific polyclonal antibodies as well as with monoclonal antibodies alone or in combination with other cartilage-binding antibodies (19,20), indicating that B cells are involved in disease development. We previously reported that mouse monoclonal antibodies (mAb) raised against COMP were not only able to promote arthritis when combined with anti–type II collagen (CII) antibody, but were also capable of inducing joint pain in naive mice (19,21). These data collectively indicate that both COMP and its autoantibodies play pathogenic roles in experimental arthritis and further indicate that they may have a potentially important role in RA. Indeed, antibodies to COMP were detected in synovium and serum from RA patients (22).

COMP plays an essential role in matrix assembly by interacting with many extracellular and cell surface proteins (14). We have previously shown that there are several epitopes, mainly located in the EGF-like repeats of COMP, that can be targeted by autoantibodies, such as 15A11 and 16B5, generated using mice with COMP-induced arthritis (19). Understanding the molecular basis for the interaction of autoantibodies with COMP as well as whether and how this interaction influences the structural features of the ECM, thereby causing cartilage damage, will thus further our understanding of the pathogenesis of rheumatic diseases. Therefore, in the present study we aimed to investigate the pathogenesis of anti-COMP antibodies in experimental arthritis at the molecular level as well as the functional role of COMP as an autoantigen in human RA.

MATERIALS AND METHODS

Reagents and more detailed methods for enzyme-linked immunosorbent assay (ELISA), histologic assessment, and surface plasma resonance measurement are described in the Supplementary Materials and Methods (available on the *Arthritis & Rheumatology* website at http://onlinelibrary.wiley.com/doi/10.1002/art.42072).

Animals. C57BL mice with an H-2^q congenic fragment (denoted B10.Q) were used in all experiments, as this genetically defined background is used as a standard background (23). In some experiments (neonatal injections), a B10.Q mouse with a *Mus musculus* Fc receptor locus (24) was used as the congenic fragment, which likely did not affect the results. All mice were housed and bred in a climate-controlled specific pathogen–free environment on 12-hour light/dark cycles, housed in polystyrene cages containing wood shavings in the animal facility of the Division of Medical Inflammation Research at the Karolinska Institute and the Central Animal Laboratory of the University of Turku. Mice were provided with standard rodent chow and water ad libitum. All experiments were performed in 8–10-week-old mice under standard conditions. The experiments were approved by the Stockholm ethics committee (approval nos. N490/12 and H2014-483) and the National Animal Experiment Board in Finland (approval no. ESAVI/439/04.10.07/2017).

Passive transfer of antibodies. Three groups of B10.Q mice were injected intravenously with either 9 mg M2139 (specific to type II collagen/Col2) (25); 9 mg 15A11 (specific to COMP) (19); or a combination of M2139 and 15A11 (4.5 mg of each). On day 5, each mouse was intraperitoneally administered 25 μg lipopolysaccharide (LPS) from the *Escherichia coli* serotype O55:B5 (Sigma-Aldrich) to increase the severity of developing arthritis. Arthritis development was monitored daily in a blinded manner for 12 days using an extended scoring protocol. Briefly, clinical arthritis was defined as swelling and redness in the joint and was scored as follows: 1 point was assigned for each swollen or red toe, 1 point was assigned for each swollen joint (metatarsophalangeal joints, metacarpophalangeal joints, proximal interphalangeal joints, and distal interphalangeal joints), and 5 points were assigned for a swollen ankle (maximum score per limb 15 points, maximum score per mouse 60 points).

Crystallization, data collection, and structure determination. Purified 15A11 Fab fragment (final concentration 10 mg/ml in 20 mM Tris HCl, pH 7.4, 50 mM NaCl) was mixed with P6 peptide with a rat-specific sequence at a molar ratio of 1:1.2. Screening for crystallization conditions was performed in a sitting-drop vapor diffusion setup at 20°C using Crystal Screen HT (Hampton Research), with 0.3-μl drops equilibrated against 60-μl reservoirs. Crystals appeared under several conditions and were tested for diffraction. The data used for structure determination were collected from a crystal obtained with screening condition C6 (30% polyethylene glycol 8000, 0.2M ammonium sulfate) and a drop mixed at a 2:1 ratio with protein and reservoir solution. The crystal was briefly soaked in a cryoprotectant consisting of

reservoir solution supplemented with 15% (volume/volume) glycerol before it was flash-frozen in liquid N_2. Crystallographic data were collected at 100K at Beamline I03 of the Diamond Light Source, indexed and integrated on-site with XIA2-3d, and scaled using Aimless from the CCP4 suite of programs (26–32).

The initial estimates of phases were obtained by molecular replacement using the program Phaser (33). We performed manual model building using Coot (34) alternating with translation, liberation, and screw-motion and restrained refinement in REFMAC5 (35). A set including 5% of randomly selected reflections was used to monitor R_{free}. Water molecules were added in Coot. Molecular surfaces were analyzed with the Protein Interfaces, Surfaces and Assemblies service at the European Bioinformatics Institute (36). Crystal structure images were prepared with PyMOL (37). The crystallographic coordinates and structure factors of the 15A11 Fab–P6 complex have been deposited in the Protein Data Bank (PDB) (no. 6SF6).

Patient cohorts. In the present study, we used the prospective observational Early Intervention in RA second cohort (TIRA-2) consisting of 504 RA patients, and healthy subjects from the Western Region Initiative to Gather Information on Atherosclerosis cohort were used as controls (n = 290). Between 2006 and 2009, RA patients enrolled in the TIRA-2 fulfilled the American College of Rheumatology 1987 criteria for RA (38) or at least the criteria of morning stiffness for ≥60 minutes, symmetric arthritis, and arthritis in the small joints (39). The study protocols were approved by the regional ethics review boards in Linköping (approval nos. TIRA-2, M168-05, and 2005-12-14) and Gothenburg (approval nos. WINGA, 676-08, and T953-15).

Luminex immunoassay. The detection of autoantibody responses using Luminex technology has been described previously (40–42). Briefly, all biotinylated peptides were captured on beads via recognition of NeutrAvidin (ThermoFisher Scientific), which was immobilized on the beads with amine coupling. Human serum samples were diluted 1:100 (v/v) in assay buffer (3% bovine serum albumin, 5% milk powder, 0.1% ProClin 300, 0.05% Tween 20, 100 µg/ml NeutrAvidin in phosphate buffered saline [PBS]) and incubated for 60 minutes at room temperature. Then the serum samples were transferred to a 384-well plate containing peptide-coated beads, with a liquid handler (CyBio Selma). After incubation at room temperature on a shaker for 75 minutes, all beads were washed with PBS-Tween (PBST) on a plate washer (no. EL406; BioTek) and resuspended in a solution containing secondary anti-human phycoerythrin-conjugated IgG Fcγ (Jackson ImmunoResearch). After 40 minutes of incubation, the beads were washed with PBST and subsequently measured in a Flexmap 3D system (Luminex). The median fluorescence intensity was used to quantify the interaction of serum antibody with given peptides.

Statistical analysis. Quantitative data from the animal experiments are expressed as the mean ± SEM. We compared antibody responses in Luminex immunoassays using a nonparametric Mann-Whitney U test. P values less than 0.05 were considered significant. The cutoff for assessing the reactivity of a given peptide in the Luminex immunoassay is the median + 5× the mean absolute deviation from healthy controls. To assess the correlation of Disease Activity Score in 28 joints (DAS28) (43) with the reactivity of P6–CIT247 at different time points, we performed a linear regression analysis by adjusting for the effects of sex, age, and shared epitope status of the patients. All statistical calculations were performed with R and various R packages (44).

RESULTS

Arthritis induction by COMP-specific antibodies in mice. We previously mapped the 15A11 binding site in the fourth EGF-like domain of murine COMP (Figure 1A) (19). The epitope comprises residues 232–252 and was designated P6. The primary sequence of the rat COMP epitope (GSPSPCHEKADCILERDGSRS) differs at 3 positions compared to human COMP (Figure 1A). Nevertheless, mAb 15A11 binds equally well to both mouse and human COMP protein (19).

It has been shown that mAb 15A11, in combination with a subarthritogenic dose of Col2-specific mAb M2139, can increase the severity of induced acute arthritis in naive mice (19). To assess the arthritogenicity of 15A11 itself, we performed antibody-induced arthritis experiments in B10.Q mice by single-dose injection of mAb 15A11. As shown in Figure 1B, a single dose of 9 mg mAb 15A11 or mAb M2139 induced arthritis, whereas, an irrelevant isotype IgG1 antibody did not induce arthritis if administered at a dose of 4 mg (Supplementary Figure 1, http://onlinelibrary.wiley.com/doi/10.1002/art.42072). Based on our previous results (19), we assumed that arthritis induction in this experiment was due to recognition of COMP by 15A11. We also observed signs of arthritis before LPS challenge in the group injected with mAb 15A11 and mAb M2139 together (Figures 1B and C), implying high arthritogenicity of these mAb in the B10.Q mouse strain.

To confirm the correlation with clinical observations, we performed a histologic assessment of synovial membrane and cartilage by examining the paws of arthritic mice after termination of the experiments. The findings indicated that synovitis, pannus formation, hyperplasia, and proteoglycan loss were present in mice with arthritis (Supplementary Figure 2, http://onlinelibrary.wiley.com/doi/10.1002/art.42072).

Cartilage binding of 15A11. To investigate whether 15A11 can bind directly to COMP in cartilage in vivo, we injected a biotinylated antibody into neonatal mice and prepared frozen sections of whole paws for immunostaining. For both in vitro and in vivo staining, we used 2-day-old neonates to avoid decalcification, which could redistribute antibodies in in vivo binding assays,
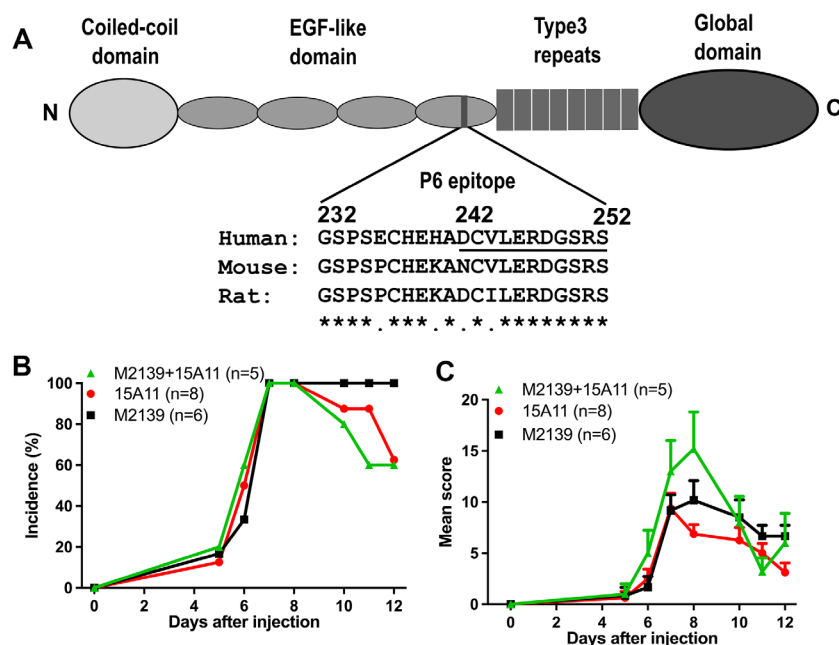
Figure 1. Arthritogenicity of cartilage oligomeric matrix protein (COMP)–specific monoclonal antibody (mAb) 15A11 in mice. **A**, Schematic presentation of the location of P6 in COMP. **B** and **C**, Incidence (**B**) and severity (**C**) of arthritis induced by passive transfer of antibodies to mice. Two-month-old naive male B10.Q mice were injected intravenously with either 9 mg of an equal combination of mAb M2139 and mAb 15A11, 9 mg of mAb M2139 alone, or 9 mg of mAb 15A11 alone. Each mouse was administered lipopolysaccharide (25 μg/mouse) intraperitoneally on day 5, and arthritis was scored daily for 12 days. Values in **C** are the mean ± SEM. EGF = epidermal growth factor. Color figure can be viewed in the online issue, which is available at http://onlinelibrary.wiley.com/doi/10.1002/art.42072/abstract.

as previously reported (45). Notably, injected antibodies can only target the cartilage surface in vivo, as the antibodies cannot penetrate very deeply into cartilage (45). For in vitro staining, all cartilage in the tissue section is accessible for staining; hence, it can be targeted by antibodies. As seen in Figure 2, we found that mAb 15A11 and anti-Col2 mAb M2139 demonstrated specific in vivo staining patterns on the lining of the articular cavity in native cartilage tissue. In contrast, tissue samples from control mice injected with PBS showed no staining. Furthermore, to investigate the binding capacity of 15A11 to cartilage in vitro, we performed an immunohistochemical analysis using frozen sections from naive neonatal mice. As seen in Figure 2, we observed strong widespread staining on cartilage for both 15A11 and M2139, while no staining was detectable in control samples. Taken together, these data show that COMP is accessible to antibodies on the cartilage surface in vivo.

Overall structure of the 15A11 Fab fragment in complex with COMP P6. In order to reveal the molecular basis of the interaction between 15A11 and COMP, we determined the crystal structure of the complex between the 15A11 Fab fragment and P6 peptide at 1.9Å resolution using molecular replacement. Data collection and refinement statistics are summarized in Supplementary Table 1 (http://onlinelibrary.wiley.com/doi/10.1002/art.42072).

The crystal structure belongs to space group $P2_12_12_1$ and contains 2 Fab–peptide complexes per asymmetric unit. Clear

and continuous electron density was visible for residues 1–216 of the light chain and residues 1–137 and 142–222 of the heavy chain in the 15A11 Fab fragments.

Clearly defined electron density was only observed in the 11 C-terminal amino acids in the P6 peptide (^{242}DCILERDGSRS^{252}), which adopt a β-hairpin–like structure in the groove formed by the complementarity-determining regions (CDRs) of the 15A11 antibody (Figure 3B). An extension of the visible density of the side chain of C243 indicated that it is oxidized to S-hydroxy cysteine in the crystal used for structure determination. The β-hairpin conformation of P6 is stabilized by a total of 7 intrapeptide hydrogen bonds that primarily involve main chain atoms (Supplementary Table 2, http://onlinelibrary.wiley.com/doi/10.1002/art.42072). S252 alone formed 4 of these bonds, 2 with I244 via its backbone amide and carbonyl group, respectively, and the other 2 with D248 and E246 via its side chain hydroxyl group. In addition to the latter, E246 formed main chain atom–mediated hydrogen bonds with G249 and S250, while the seventh hydrogen bond linked the side chain of D248 with the backbone amide of S250. The N-terminal half of P6, which extended out of the binding groove into the surrounding solvent, can adopt multiple different conformations as indicated by the complete lack of electron density.

Interactions between the 15A11 Fab fragment and P6. Formation of the antibody–antigen complex covered ~47%
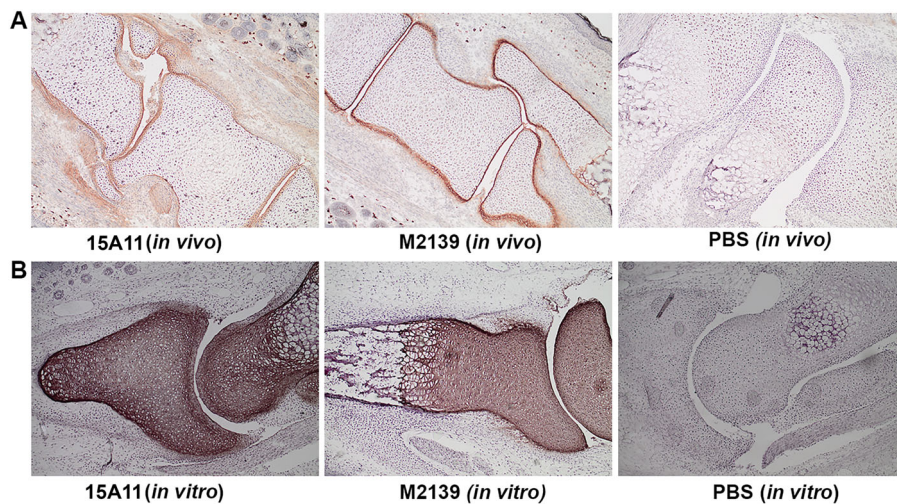
Figure 2. Specificity of mAb 15A11 binding to joint cartilage in vivo and in vitro. **A**, For histologic detection of the binding of mAb 15A11 to cartilage in vivo, a single dose of 100 μg of biotinylated anti-COMP mAb 15A11 was injected into 2-day-old neonatal BQ.Cia9i mice, and limbs were collected after 48 hours to make 5-μm cryosections. **B**, For in vitro analysis of the interaction between mAb 15A11 and cartilage, an immunohistochemical assay was performed on the 5-μm limb cryosections. Staining was performed with diaminobenzidine using ExtrAvidin–peroxidase as a detection system. Mice injected with biotinylated anti-Col2 mAb (M2139) and phosphate buffered saline (PBS) were used as a positive reference and blank control, respectively. Results shown are representative of 2–3 mice per group. Original magnification × 10. See Figure 1 for other definitions.
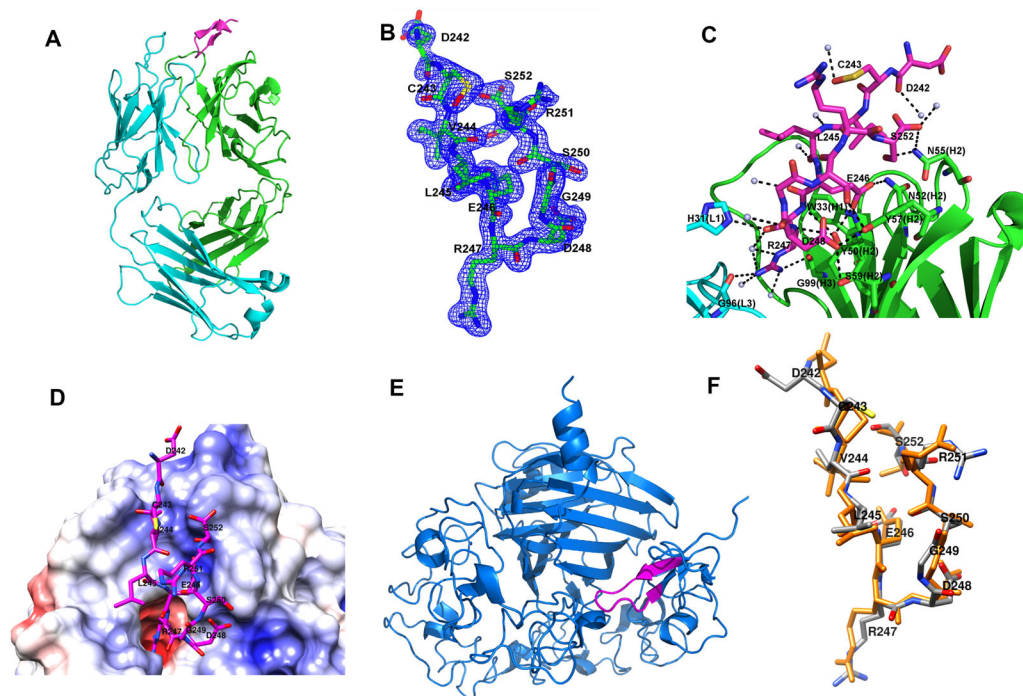
Figure 3. Crystal structure of the mAb 15A11–Fab complex. **A**, Overall complex of 15A11 Fab bound to COMP P6 peptide. The 15A11 Fab light chain (cyan) and heavy chain (green) are shown. **B**, Electron density map for the P6 peptide. The final $2F_o–F_c$ difference map is contoured at a contour level of 1σ. **C**, Close-up stereoscopic view of the 15A11 paratope with bound P6 peptide. Fab residues and peptide residues (black) are distinguished by color. Water molecules (red) and hydrogen bonds (broken lines) are shown. **D**, Close-up stereoscopic view of the 15A11 paratope in surface presentation, with bound peptide shown. Colors of the paratope surface indicate the electrostatic potential as calculated using PyMOL. P6 residue R247 is deeply buried in a narrow pocket. **E**, P6 epitope–based superimposition of the crystal structure of truncated COMP (Protein Data Bank entry no. 3FBY [blue] with the P6 epitope [magenta]). **F**, Comparison of the conformations of 15A11-bound P6 peptide (yellow carbon atoms) and the P6 epitope within crystallized truncated COMP (magenta carbon atoms). See Figure 1 for other definitions.

(~640Å^2) and 2.5 % (~470Å^2) of the solvent-accessible surface area of the P6 peptide and the 15A11 Fab, respectively (Supplementary Tables 3 and 4, http://onlinelibrary.wiley.com/doi/10.1002/art.42072). The ^{244}ILERD^{248} motif of the peptide contributed the most to the interface, with additional significant contributions by C243, G249, S250, and S252, while D242 contacted the Fab exclusively via a water-mediated hydrogen bond to N55 from the heavy chain (Figure 3C). The only peptide residue with clearly visible electron density that was not involved in interactions with the 15A11 Fab fragment was R251. It was entirely solvent exposed and thus accessible to residues of a symmetry-related Fab fragment, with which it formed 3 hydrogen bonds via its main chain atoms. In the 15A11 Fab fragment, all CDRs except L2 were involved in epitope recognition, and H2 and H3 are the primary contact regions.

P6 epitope binding by Fab led to the formation of 11 direct and 7 water-mediated hydrogen bonds (Figure 3C and Supplementary Table 2, http://onlinelibrary.wiley.com/doi/10.1002/art.42072), as well as several hydrophobic and van der Waals interactions. These interactions were centered around E246 and R247, which are both entirely buried upon interface formation. The long side chain of R247 was inserted into a narrow, deep pocket in the center of the binding groove. Its entrance was formed by hydrophobic residues from both heavy chain and light chain CDRs, while increasing polarity and placement of E39 (light chain) at its deepest point provided shape and charge complementarity for recognition of R247 (Figure 3D). However, the depth of the pocket led to the formation of 2 water-mediated hydrogen bonds rather than a salt bridge with E39, which may explain why the mAb also efficiently recognized citrullinated P6 epitopes (see below). In addition, R247 was linked to G96 (L3), Y50 (H2), G99 (H3), H31 (L1), and W108 (H3) via direct or water-mediated hydrogen bonds, accounting for 8 of 18 total polar contacts between the P6 peptide and 15A11 Fab. Recognition of P6–E246 was mediated by an additional 4 hydrogen bonds, N52 and Y50 from the H2 CDR, W33 from H1, and H31 from the L1 CDR.

Of the P6 positions contacted by the mAb 15A11, all but 1 were conserved in rat, mouse, and human COMP sequences, explaining the observed cross-recognition (Figure 1A). The exception was I244, which was conservatively exchanged by valine in human COMP and mouse COMP. However, the absence of the additional methyl group likely has little influence on binding specificity and strength, as it indicates a more solvent-exposed region of the paratope and thus most likely does not significantly contribute to the interactions.

Structure of the P6 epitope in native COMP. To understand why mAb 15A11 can bind to native COMP and the P6 peptide, we compared the structure of the 15A11-bound peptide (rat sequence) to the native epitope within human COMP (PDB no. 3FBY). As shown in Figure 3E, the P6 epitope was

located near the N-terminal of the crystallized truncated construct, which contained the last EGF-like repeat, the type III repeats, and the C-terminal domain of human COMP. As in the 15A11 Fab complex, it adopted a β-hairpin conformation (Figure 3F). The backbone root mean square deviation of the superimposition of the Cα atoms of residues 242–252 of the 15A11-bound and native P6 epitope was 0.63–0.80Å, which indicates that the conformation of the epitope itself remains largely unaltered upon interaction with mAb 15A11, allowing direct recognition both in vivo and in vitro. However, binding of 15A11 would require conformational changes in COMP to make the P6 epitope more accessible than in the crystallized construct, as serious clashes occur between the Fab and the C-terminal domains of the COMP protein superimposed peptides in both crystal structures. It has been suggested that the positioning/orientation and the conformation of this domain in COMP protein are affected by cations (46).

Modulation of 15A11 binding to COMP by calcium ions. Since binding of calcium ions to COMP alters the conformation of the individual domains and thereby the interaction between COMP and various substrates (46), we hypothesized that this might also affect binding of mAb 15A11 to native COMP. Therefore, we performed an ELISA to measure the binding behavior of 15A11 at different Ca^{2+} concentrations. As shown in Figure 4A, mAb 15A11 binding to COMP was calcium dependent, while binding of another COMP-specific mAb, 16B, was calcium independent.

We also measured the binding affinity of mAb 15A11 for COMP by surface plasmon resonance with or without the addition of 10 mM Ca^{2+}. Since the algorithm we used could not fit our experimental data with the default parameter values, we could not obtain reliable kinetics values. However, we obtained the steady-state affinity (K_d) value by fitting the binding curves shown in Figures 4B and C. The mAb 15A11 showed slightly stronger binding to COMP in the absence of calcium (K_d = 173.6 nM) than in the presence of calcium (K_d = 413.8 nM). In particular, the level of binding response (resonance units) in the presence of calcium ions was significantly higher than without calcium (Figures 4B and C), indicating that there were more COMP molecules captured by the 15A11-immobilized sensor chip. These data demonstrate that the Ca^{2+} concentration can modulate the binding strength of mAb 15A11 to COMP, most likely by affecting the conformation of the fourth EGF-like repeat, making the P6 epitope more accessible. Interestingly, we found that 15A11 had comparable binding capability toward P6–CIT247 and P6–R247 (Figure 4D), which can be explained by the negatively charged binding pocket in residue 247.

Identification of P6 as an immunodominant B cell epitope in RA patients. To assess the prevalence of anti-P6 antibodies and their association with RA, we measured antibody
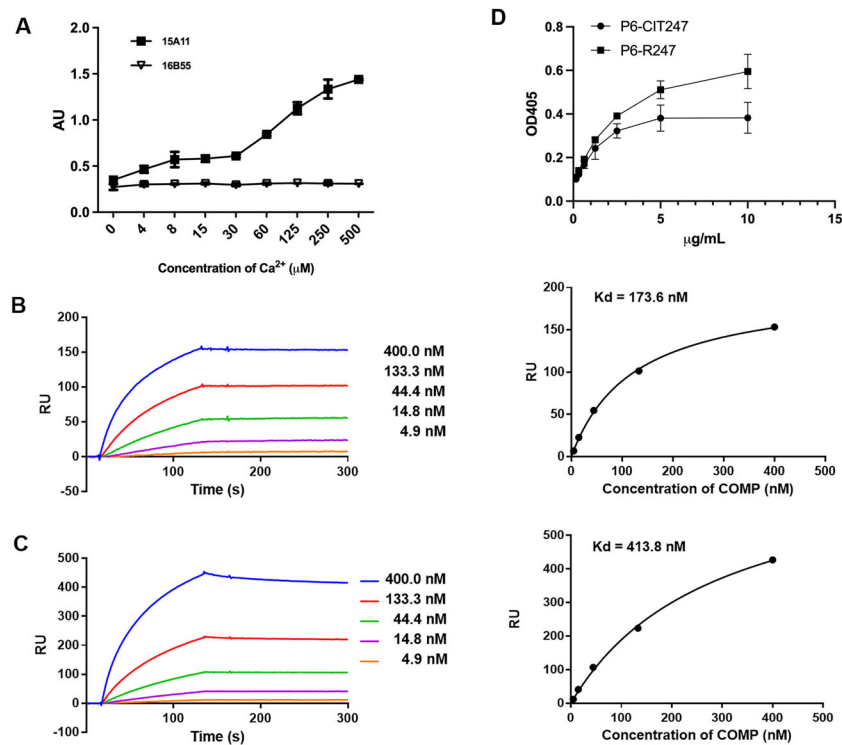
Figure 4. Modulation of binding by calcium. **A**, Influence of calcium ions on the interaction between mAb 15A11 and COMP, measured by enzyme-linked immunosorbent assay (ELISA). COMP-specific mAb 16B was used as a control. **B** and **C**, Association and dissociation curves for the interaction of 15A11 with COMP with (**C**) or without (**B**) 10 mM CaCL$_2$, measured by surface plasmon resonance. **D**, Binding of 15A11 to P6–CIT247 or P6–R247, measured by ELISA. Values in **A** and **D** are the mean $\pm$ SEM. RU = resonance unit (see Figure 1 for other definitions). Color figure can be viewed in the online issue, which is available at http://onlinelibrary.wiley.com/doi/10.1002/art.42072/abstract.

responses to the P6 peptide in a Swedish cohort consisting of 504 patients with early untreated RA and 290 healthy controls, using Luminex immunoassay. Both linear and cyclic P6 unmodified peptides (P6–R-R and P6–R247, respectively) were immobilized on magnetic beads to measure antibody responses. Similarly, to study the citrulline dependence of the antibody response to this epitope, we also analyzed 3 citrullinated linear peptides (P6–R-CIT, P6–CIT-R, and P6–CIT-CIT) and 1 citrullinated cyclic peptide (P6–CIT247). As shown in Figure 5, statistically significant antibody reactivity toward all P6 peptide variants was detected in RA patients compared to healthy controls ($P < 0.001$). Regarding the linear forms of the P6 epitope, autoantibody responses to the 3 citrullinated variants P6–R-CIT ($P = 1.13 \times 10^{-10}$), P6–CIT-R ($P = 6.37 \times 10^{-10}$), and P6–CIT-CIT ($P = 4.11 \times 10^{-9}$) were more significant than the response to the unmodified form P6–R-R ($P = 8.24 \times 10^{-3}$). Similarly, the cyclic form of the citrullinated P6 epitope P6–CIT247 demonstrated much higher reactivity in RA patients than its unmodified form P6–R247 ($P = 5.72 \times 10^{-3}$ and $P = 2.47 \times 10^{-33}$, respectively).

Among all peptides, P6–CIT247 had the highest prevalence (38%). In comparison, we also measured the prevalence of antibody responses to 2 classic citrullinated peptides, citrullinated peptide 1 (CCP-1) and citrullinated α-enolase peptide 1 (CEP-1), in the same cohort. CCP-1 and CEP-1 were found in 57% and

56% of patients, respectively, which is comparable to previously reported results (47,48). Although most RA patients who were positive for P6–CIT247 antibody were also positive for CEP-1 and CCP-1, ~8% of the patients were positive for P6–CIT247 only (Figure 6). Interestingly, the cyclic form of the P6 epitope demonstrated much higher reactivity than the corresponding linear form, possibly because the β-hairpin conformation required for recognition is better stabilized in cyclic peptides (see above).

More importantly, we evaluated potential associations between autoantibody specificity and DAS28 scores over time using multivariate regression analysis with adjustment for the effects of sex, age, and shared epitope allele status. As shown in Supplementary Table 5 (http://onlinelibrary.wiley.com/doi/10.1002/art.42072), patients who responded to P6–CIT247 appeared to have more severe disease activity at 12 months ($P = 0.051$) and 24 months ($P = 0.029$) after diagnosis compared to those who did not respond to P6–CIT247.

DISCUSSION

In this study, we investigated the properties of a COMP-specific antibody that recognizes native COMP protein in joint cartilage, causing arthritis after injection into mice. The pathogenicity of anti-COMP antibodies is likely relevant in humans, and the
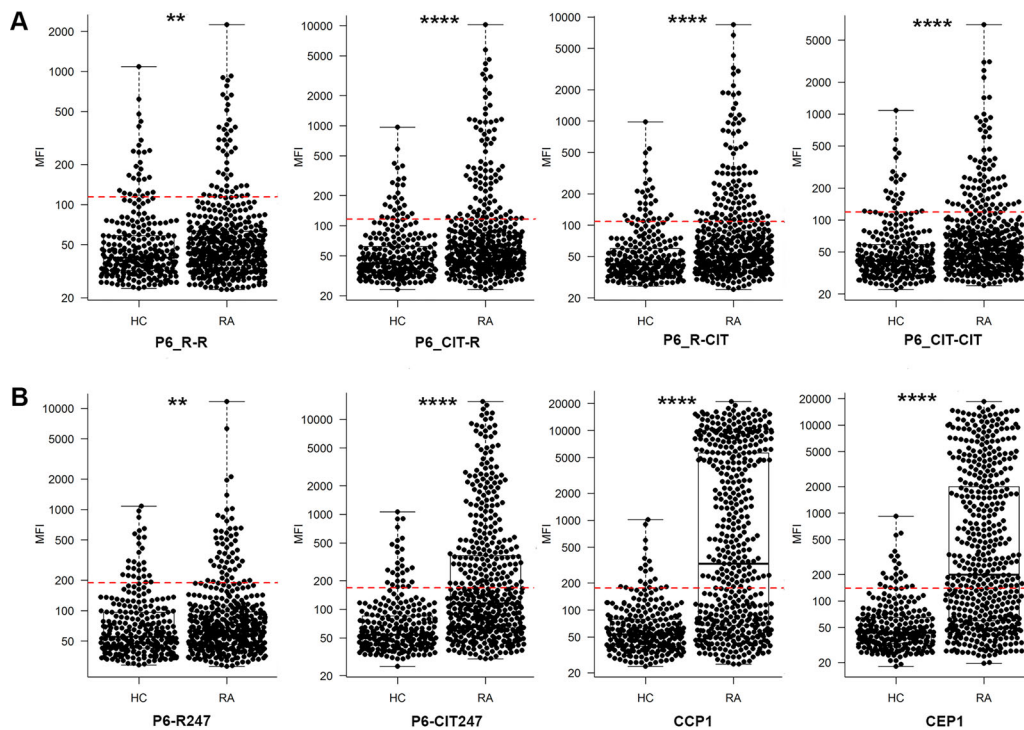
Figure 5. Human serum IgG response to P6 peptide variants in patients with rheumatoid arthritis (RA) compared to healthy controls (HC). IgG responses to linear (**A**) and cyclic (**B**) forms of the P6 epitope are shown. Citrullinated peptides P6–R-CIT, P6–CIT-R, P6–CIT-CIT, and P6–CIT247 showed higher positive responses than the noncitrullinated peptides P6–R-R (linear) and P6–R247 (cyclic). IgG levels were measured by Luminex assay. Symbols represent the reactivity of individual serum samples with the indicated peptide; bars show the mean ± SEM. Boxed areas denote box plots, where the boxes represent the 25th to 75th percentiles, the lines within the boxes represent the median, and the lines outside the boxes represent the 10th and 90th percentiles. Dashed red lines show the cutoffs for positivity, defined as the median + 5× the mean absolute deviation in median fluorescence intensity (MFI) values in the healthy controls. ** = $P < 0.01$; **** = $P < 0.0001$, by Mann-Whitney U test. CCP-1 = citrullinated peptide 1; CEP-1 = citrullinated α-enolase peptide 1. Color figure can be viewed in the online issue, which is available at http://onlinelibrary.wiley.com/doi/10.1002/art.42072/abstract.

antibody cross-reacts with human COMP. Furthermore, antibodies reacting with both native and citrullinated variants of COMP are indeed detectable in RA. To elucidate the molecular determinants by which arthritogenic mAb 15A11 specifically recognizes

COMP in joint cartilage, we determined the crystal structure of its Fab fragment in complex with the P6 epitope, which according to findings from our previous epitope mapping study, spans residues 232–252 of mouse COMP (19). The interactions observed
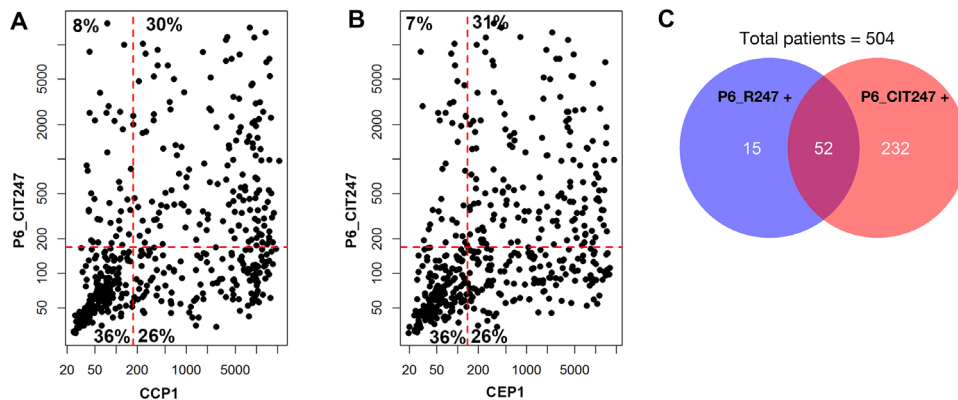
Figure 6. Autoantibodies against P6–CIT247 are highly associated with autoantibodies toward other citrullinated peptides. **A** and **B**, Rheumatoid arthritis patient–derived autoantibodies reactive with P6–CIT247 in relation to those responding to either citrullinated peptide 1 (CCP-1) (**A**) or citrullinated α-enolase peptide 1 (CEP-1) (**B**). Dashed lines show the cutoffs for positivity, defined as the median + 5× the mean absolute deviation from corresponding healthy controls. **C**, Venn diagram showing overlap of responses to P6–R247 and to P6–CIT247. Color figure can be viewed in the online issue, which is available at http://onlinelibrary.wiley.com/doi/10.1002/art.42072/abstract.

between the 15A11 antibody and P6 epitope in the crystal structure explain how this antibody can cross-react with the native COMP protein, thereby binding cartilage in vivo and efficiently inducing arthritis and joint pain. Binding is mainly governed by paratope shape–complementarity to the epitope in a β-hairpin conformation and the availability of a deep, narrow, and appropriately charged binding pocket for residue R247 of P6. When the structure of the P6 peptide bound to the 15A11 Fab fragment is superimposed onto the corresponding sequence in the COMP crystal structure, it becomes apparent that recognition of native COMP by mAb requires an increase in accessibility more than conformational changes in the epitope. The sequence dependency of epitope recognition is further highlighted by the fact that almost all residues of P6 visible in the crystal structure are conserved in human, mouse, and rat COMP, with the only exception representing a conservative exchange of residues.

Degradation of COMP and associated ECM constituents is mainly mediated by ADAMTS proteins and matrix metalloproteinase 13 (14) targeting the 4 evolutionarily conserved EGF-like repeats (49,50). Also, other COMPs interact with the EGF-like domain. Their interaction with cells through integrins could potentially affect cell adhesion during immune responses as well as in apoptosis (51,52).

It has also been shown that injection of a set of monoclonal IgG antibodies against COMP induces arthritis and enhances the development of cartilage antibody–induced arthritis when combined with anti-Col2 IgG antibodies (19). This study shows that a single injection of mAb 15A11 alone is sufficient to mount an immune response in naive mice and induce severe arthritis. This supports the notion that autoantibodies to COMP can play a pathogenic role in experimental arthritis by directly binding to exposed surface epitopes of COMP in joint cartilage, resulting in tissue damage (see Figure 2 and Supplementary Figure 1, http://onlinelibrary.wiley.com/doi/10.1002/art.42072). Hence, COMP antibodies act similarly to autoantibodies toward Col2, which are also well known to be pathogenic in mice by interacting directly with the native triple-helical conformation of Col2 in cartilage (53).

In addition to its pathogenic role in mice, COMP might also be important as a biomarker for disease activity and joint destruction in RA (15). Increased COMP fragments are detectable in serum and synovial fluid in RA and other inflammatory and degenerative diseases such as OA and systemic sclerosis (15). However, our current knowledge about autoimmunity to COMP in RA is limited.

Since the P6 epitope is a major pathogenic epitope in COMP-induced arthritis in mice and is conserved in humans, we tested the antibody response in RA. Interestingly, we detected a significant response not only to the native epitope but also to the citrullinated P6 epitope. Similar to Col2, antibodies recognizing native COMP epitopes are less frequently observed compared to their citrullinated counterparts. The higher frequency of

citrullinated COMP–reactive antibodies may explain in part why antibodies specifically interacting with citrulline could promiscuously respond to many different peptides (54,55). However, a minor, potentially pathogenic fraction of antibodies could more specifically recognize citrullinated and native COMP within cartilage and thereby mediate arthritis.

Interestingly, COMP fragments are released into body fluids such as synovial fluid and blood (15). Joint synovium and synovial fluid contain peptidylarginine deiminases (PADs), which catalyze the modification of arginine to citrulline (56). Hence, the P6 epitope (and probably other unknown COMP fragments) are more likely to be modified by extracellular PADs, leading to neoantigens providing targets for antibodies.

The observed critical role of Ca^{2+} ions in the 15A11–COMP interaction was dose dependent. It is most likely mediated via conformational changes in COMP, as in silico docking of 15A11 Fab onto the P6 epitope in the crystal structure of (truncated) COMP in the absence of Ca^{2+} ions revealed that the epitope would otherwise be inaccessible to mAb 15A11. It has been shown that the pentameric form of COMP exists in a more compact conformation in the presence of Ca^{2+} (14,44). Interestingly, this finding raises the possibility that an increased extracellular level of calcium in inflamed joints could lead to increased accessibility of targeted epitopes of native COMP and increased in situ citrullination. This could lead to the joint-specific formation of local immune complexes playing essential roles in increasing joint pain and inducing arthritis.

In summary, our findings provide a structural basis for understanding the pathogenic effect of an autoantibody that specifically targets a selected protein domain in native COMP accessible in joints. This could also have functional importance in RA, as this antibody, together with antibodies to citrullinated variants of the same epitope, are detectable in RA serum and may be associated with increased disease activity. These findings warrant further study of anti-COMP antibodies as potential biomarkers in RA.

REFERENCES

1. McInnes IB, Schett G. The pathogenesis of rheumatoid arthritis [review]. N Engl J Med 2011;365:2205–19.

2. Sangha O. Epidemiology of rheumatic diseases. Rheumatology (Oxford) 2000;39 Suppl:3–12.

3. Klareskog L, Catrina AI, Paget S. Rheumatoid arthritis. Lancet 2009; 373:659–72.

4. Stastny P. Association of the B-cell alloantigen DRw4 with rheumatoid arthritis. N Engl J Med 1978;298:869–71.

5. Tuomi T, Heliovaara M, Palosuo T, Aho K. Smoking, lung function, and rheumatoid factors. Ann Rheum Dis 1990;49:753–6.

6. Okada Y, Wu D, Trynka G, Raj T, Terao C, Ikari K, et al. Genetics of rheumatoid arthritis contributes to biology and drug discovery. Nature 2014;506:376–81.

7. Thorn J. The inflammatory response in humans after inhalation of bacterial endotoxin: a review. Inflamm Res 2001;50:254–61.

8. Christiani DC, Wang XR, Pan LD, Zhang HX, Sun BX, Dai H, et al. Longitudinal changes in pulmonary function and respiratory symptoms in cotton textile workers. A 15-yr follow-up study. Am J Respir Crit Care Med 2001;163:847–53.

9. Stolt P, Kallberg H, Lundberg I, Sjogren B, Klareskog L, Alfredsson L, et al. Silica exposure is associated with increased risk of developing rheumatoid arthritis: results from the Swedish EIRA study. Ann Rheum Dis 2005;64:582–6.

10. Scherer HU, Huizinga TW, Kronke G, Schett G, Toes RE. The B cell response to citrullinated antigens in the development of rheumatoid arthritis. Nat Rev Rheumatol 2018;14:157–69.

11. Oldberg A, Antonsson P, Lindblom K, Heinegård D. COMP (cartilage oligomeric matrix protein) is structurally related to the thrombospondins. J Biol Chem 1992;267:22346–50.

12. Smith R, Zunino L, Webbon P, Heinegård D. The distribution of cartilage oligomeric matrix protein (COMP) in tendon and its variation with tendon site, age and load. Matrix Biol 1997;16:255–71.

13. Tan K, Duquette M, Joachimiak A, Lawler J. The crystal structure of the signature domain of cartilage oligomeric matrix protein: implications for collagen, glycosaminoglycan and integrin binding. FASEB J 2009;23:2490–501.

14. Acharya C, Yik JH, Kishore A, Van Dinh V, Di Cesare PE, Haudenschild DR. Cartilage oligomeric matrix protein and its binding partners in the cartilage extracellular matrix: interaction, regulation and role in chondrogenesis. Matrix Biol 2014;37:102–11.

15. Tseng S, Reddi AH, Di Cesare PE. Cartilage Oligomeric Matrix Protein (COMP): a biomarker of arthritis. Biomark Insights 2009;4: 33–44.

16. Happonen KE, Saxne T, Aspberg A, Mörgelin M, Heinegård D, Blom AM. Regulation of complement by cartilage oligomeric matrix protein allows for a novel molecular diagnostic principle in rheumatoid arthritis. Arthritis Rheum 2010;62:3574–83.

17. Carlsén S, Hansson AS, Olsson H, Heinegård D, Holmdahl R. Cartilage oligomeric matrix protein (COMP)-induced arthritis in rats. Clin Exp Immunol 1998;114:477–84.

18. Carlsen S, Nandakumar KS, Bäcklund J, Holmberg J, Hultqvist M, Vestberg M, et al. Cartilage oligomeric matrix protein induction of chronic arthritis in mice. Arthritis Rheum 2008;58:2000–11.

19. Geng H, Nandakumar KS, Pramhed A, Aspberg A, Mattsson R, Holmdahl R. Cartilage oligomeric matrix protein specific antibodies are pathogenic. Arthritis Res Ther 2012;14:R191.

20. Li Y, Tong D, Liang P, Lonnblom E, Viljanen J, Xu B, et al. Cartilage-binding antibodies initiate joint inflammation and promote chronic erosive arthritis. Arthritis Res Ther 2020;22:120.

21. Farinotti AB, Wigerblad G, Nascimento D, Bas DB, Urbina CM, Nandakumar KS, et al. Cartilage-binding antibodies induce pain through immune complex-mediated activation of neurons. J Exp Med 2019;216:1904–24.

22. Souto-Carneiro MM, Burkhardt H, Muller EC, Hermann R, Otto A, Kraetsch HG, et al. Human monoclonal rheumatoid synovial B lymphocyte hybridoma with a new disease-related specificity for cartilage oligomeric matrix protein. J Immunol 2001;166:4202–8.

23. Ahlqvist E, Ekman D, Lindvall T, Popovic M, Forster M, Hultqvist M, et al. High-resolution mapping of a complex disease, a model for rheumatoid arthritis, using heterogeneous stock mice. Hum Mol Genet 2011;20:3031–41.

24. Vaartjes D, Klaczkowska D, Cragg MS, Nandakumar KS, Backdahl L, Holmdahl R. Genetic dissection of a major haplotype associated with arthritis reveal FcγR2b and FcγR3 to act additively. Eur J Immunol 2021;51:682–93.

25. Raposo B, Dobritzsch D, Ge C, Ekman D, Xu B, Lindh I, et al. Epitope-specific antibody response is controlled by immunoglobulin V(H) polymorphisms. J Exp Med 2014;211:405–11.

26. Winter G. Xia2: an expert system for macromolecular crystallography data reduction. J Appl Crystallogr 2010;43:186–90.

27. Zhang Z, Sauter NK, van den Bedem H, Snell G, Deacon AM. Automated diffraction image analysis and spot searching for high-throughput crystal screening. J Appl Crystallogr 2006;39:112–9.

28. Sauter NK, Grosse-Kunstleve RW, Adams PD. Robust indexing for automatic data collection. J Appl Crystallogr 2004;37:399–409.

29. Kabsch W. Xds. Acta Crystallogr D Biol Crystallogr 2010;66:125–32.

30. Evans P. Scaling and assessment of data quality. Acta Crystallogr D Biol Crystallogr 2006;62:72–82.

31. Collaborative Computational Project N. The CCP4 suite: programs for protein crystallography. Acta Crystallogr D Biol Crystallogr 1994;50:760–3.

32. Evans PR, Murshudov GN. How good are my data and what is the resolution? Acta Crystallogr D Biol Crystallogr 2013;69:1204–14.

33. Mccoy AJ, Grosse-Kunstleve RW, Adams PD, Winn MD, Storoni LC, Read RJ. Phaser crystallographic software. J Appl Crystallogr 2007; 40:658–74.

34. Emsley P, Lohkamp B, Scott WG, Cowtan K. Features and development of Coot. Acta Crystallogr D Biol Crystallogr 2010;66:486–501.

35. Murshudov GN, Vagin AA, Dodson EJ. Refinement of macromolecular structures by the maximum-likelihood method. Acta Crystallogr D Biol Crystallogr 1997;53:240–55.

36. Krissinel E, Henrick K. Inference of macromolecular assemblies from crystalline state. J Mol Biol 2007;372:774–97.

37. DeLano WL. The PyMOL molecular graphics system, version 1.2r3pre, Schrödinger, LLC. 2002.

38. Arnett FC, Edworthy SM, Bloch DA, McShane DJ, Fries JF, Cooper NS, et al. The American Rheumatism Association 1987 revised criteria for the classification of rheumatoid arthritis. Arthritis Rheum 1988;31: 315–24.

39. Svärd A, Skogh T, Alfredsson L, Ilar A, Klareskog L, Bengtsson C, et al. Associations with smoking and shared epitope differ between IgA- and IgG-class antibodies to cyclic citrullinated peptides in early rheumatoid arthritis. Arthritis Rheumatol 2015;67:2032–7.

40. Ayoglu B, Haggmark A, Khademi M, Olsson T, Uhlen M, Schwenk JM, et al. Autoantibody profiling in multiple sclerosis using arrays of human protein fragments. Mol Cell Proteomics 2013;12:2657–72.

41. Schwenk JM, Gry M, Rimini R, Uhlen M, Nilsson P. Antibody suspension bead arrays within serum proteomics. J Proteome Res 2008;7: 3168–79.

42. Hamsten C, Neiman M, Schwenk JM, Hamsten M, March JB, Persson A. Recombinant surface proteomics as a tool to analyze humoral immune responses in bovines infected by mycoplasma mycoides subsp mycoides small colony type. Mol Cell Proteomics 2009;8:2544–54.

43. Prevoo ML, van 't Hof MA, Kuper HH, van Leeuwen MA, van de Putte LB, van Riel PL. Modified disease activity scores that include twenty-eight–joint counts: development and validation in a prospective longitudinal study of patients with rheumatoid arthritis. Arthritis Rheum 1995;38:44–8.

44. Team RC. R: a language and environment for statistical computing. Vienna, Austria: R Foundation for Statistical Computing; 2021.

45. Holmdahl R, Jansson L, Larsson A, Jonsson R. Arthritis in DBA/1 mice induced with passively transferred type II collagen immune serum. Immunohistopathology and serum levels of anti-type II collagen auto-antibodies. Scand J Immunol 1990; 31:147–57.

46. Thur J, Rosenberg K, Nitsche DP, Pihlajamaa T, Ala-Kokko L, Heinegard D, et al. Mutations in cartilage oligomeric matrix protein causing pseudoachondroplasia and multiple epiphyseal dysplasia affect binding of calcium and collagen I, II, and IX. J Biol Chem 2001; 276:6083–92.

47. Lundberg K, Kinloch A, Fisher BA, Wegner N, Wait R, Charles P, et al. Antibodies to citrullinated α-enolase peptide 1 are specific for rheumatoid arthritis and cross-react with bacterial enolase. Arthritis Rheum 2008;58:3009–19.

48. Schellekens GA, de Jong BA, van den Hoogen FH, van de Putte LB, van Venrooij WJ. Citrulline is an essential constituent of antigenic determinants recognized by rheumatoid arthritis-specific autoantibodies. J Clin Invest 1998;101:273–81.

49. Liu CJ, Kong W, Xu K, Luan Y, Ilalov K, Sehgal B, et al. ADAMTS-12 associates with and degrades cartilage oligomeric matrix protein. J Biol Chem 2006;281:15800–8.

50. Liu CJ, Kong W, Ilalov K, Yu S, Xu K, Prazak L, et al. ADAMTS-7: a metalloproteinase that directly binds to and degrades cartilage oligomeric matrix protein. FASEB J 2006;20:988–90.

51. Kansas GS, Saunders KB, Ley K, Zakrzewicz A, Gibson RM, Furie BC, et al. A role for the epidermal growth factor-like domain of P-selectin in ligand recognition and cell adhesion. J Cell Biol 1994; 124:609–18.

52. Park SY, Kim SY, Jung MY, Bae DJ, Kim IS. Epidermal growth factor-like domain repeat of stabilin-2 recognizes phosphatidylserine during cell corpse clearance. Mol Cell Biol 2008;28:5288–98.

53. Holmdahl R, Mo JA, Jonsson R, Karlstrom K, Scheynius A. Multiple epitopes on cartilage type II collagen are accessible for antibody binding in vivo. Autoimmunity 1991;10:27–34.

54. Ge C, Holmdahl R. The structure, specificity and function of anti-citrullinated protein antibodies [review]. Nat Rev Rheumatol 2019;75: 503–8.

55. Ge C, Xu B, Liang B, Lönnblom E, Lundström SL, Zubarev RA, et al. Structural basis of cross-reactivity of anti-citrullinated protein antibodies. Arthritis Rheumatol 2019;71:210–21.

56. Kinloch A, Lundberg K, Wait R, Wegner N, Lim NH, Zendman AJ, et al. Synovial fluid is a site of citrullination of autoantigens in inflammatory arthritis. Arthritis Rheum 2008;58:2287–95.